Journal of Engineering Sciences and Innovation
Volume 3, Issue 4 / 2018, pp. 299 - 312

Technical Sciences
Academy of Romania
www.jesi.astr.ro

A. Mechanical Engineering

Received ***14 September 2018*** *Accepted* ***15 November 2018***
Received in revised from ***26 October 2018***

Fabrication and characterization of LDPE and HDPE filaments for 3D printing

NICOLETA-VIOLETA STANCIU[1], FELICIA STAN[1], CATALIN FETECAU[1*], ALEXANDRU SERBAN[2]

[1]*Center of Excellence Polymer Processing, Dunarea de Jos University, Galati, Romania*
[2]*POLITEHNICA University of Bucharest, Bucharest, Romania*

Abstract. Filament material is an important factor to be considered in the product development by 3D printing, since it can affect not only the quality but also the functionality of the printed parts. Thus, the objective of this paper is to investigate how feasible would be to use low- and high-density polyethylene to fabricate 3D printing filaments. Since the extrusion process depends on the rheological behavior of the polymers, first, the melt viscosity of LDPE and HDPE was analyzed by capillary rheology. Then, LDPE and HDPE filaments of 1.75 mm diameter were extruded under different processing conditions and subjected to tensile tests to determine the mechanical properties. Results showed that the LDPE and HDPE are suitable for manufacturing 3D printing filaments if the extrusion processing conditions are optimized.

Keywords. Rheology, filaments, low density polyethylene, high density polyethylene, 3D printing.

1. Introduction

In the last years, 3D printing technologies have been used in different industrial applications, including automotive, aerospace and healthcare (prosthetics, bone implants) [1-6]. However, the most popular applications of 3D printing are related to prototyping (55%) and fabrication (43%) [7]. 3D printing predominantly targets the production of polymeric parts. Global 3D printer market size went from $2.5 billion in 2013 to $7.3 billion in 2017 and by the end of 2018 the annual revenues from the global 3D printing market were estimated at $14 billion [7]. However, development of the 3D printing is restricted by the small number of commercially available 3D

[*]Correspondence address: Catalin.Fetecau@ugal.ro

printing filaments (PLA, ABS, and PET). Thus, fabrication of filaments from unused-by-now materials opens up a new avenue for printing of 3D components with high stiffness and strength. Thus, in this paper, the feasibility of using low- and high-density polyethylene as 3D printing materials is investigated.

2. Materials and methods

Two commercial grades of polyethylene were used, namely a low density polyethylene (LDPE ROPOTEN® T FV-20-205-3, Lukoil Bulgaria, with a peak melting and crystallization temperature of 115.9°C and 95.3°C, respectively [8]) and a high density polyethylene (HDPE 277-73, JSC KazanOrgSintez Russia, with a peak melting and crystallization temperature of 136.5°C and 113.2°C, respectively [8]).

Melt shear viscosity is a key parameter that has to be considered for manufacturing of filaments. On the other hand, melt shear viscosity is important for 3D printing since die swell can directly affect the quality of the 3D printed parts. Thus, rheological properties of LDPE and HDPE were investigated using a high-pressure capillary rheometer (Rheograph 75, Gottfert Inc., Germany) equipped with three capillary dies with length-to-diameter ratio of 10/1, 20/1, and 30/1. The rheological experiments were carried out at different temperatures (180, 190, 200, 215, 235 and 255°C) and shear rates from 50 to 5000 s^{-1}.

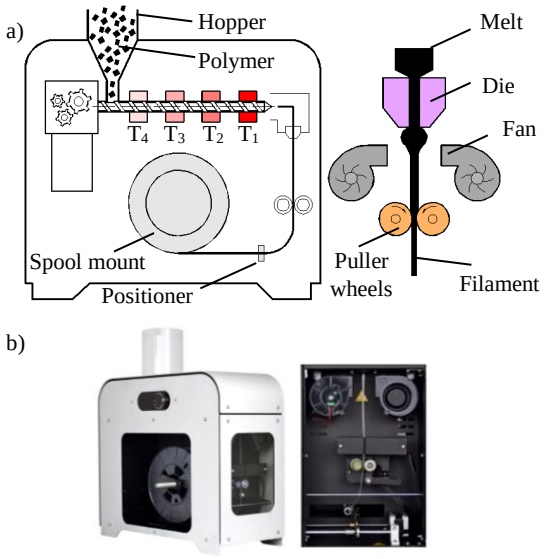

Fig. 1. a) Schematic of the filament extrusion process and b) Advanced Silver Filament extruder.

The filaments were produced using an Advanced Silver Filament extruder (3devo, Netherlands) equipped with an optical sensor and puller wheels to measure and stabilize the diameter of 1.75 mm. The extrusion process is schematically presented

in figure 1: the polymer is placed in the hopper, which feeds the extruder, passing by 4 heating zones; the melt goes through the die, which is cooled down by the fans, then the puller wheels controls the diameter of the filament; the filament is then stored on a spool mount by movement of the positioner. The filament diameter was controlled by adjusting the melt temperature and speed as indicated in Table 1. The fan speed was set to 25 % and 15% for LDPE and HDPE, respectively.

Table 1. Experimental conditions for LDPE and HDPE filament extrusion.

Material		**Speed [rpm]**	**Temperatures (°C)**			
			T_4	T_3	T_2	T_1
LDPE	L_1	2.5	185	190	195	205
	L_2	2.6			200	220
HDPE	H_1	2.2	205	210	215	225
	H_2	3			220	240

The surface quality of the extruded filaments was investigated using the optical microscopy analysis (SZX10 stereo-microscope, Olympus, Japan).
The LDPE and HDPE extruded filaments were subjected to tensile tests in order to determine the mechanical properties. Tensile tests on filaments were carried out on a Testometric universal testing machine (Model M350-5AT, UK) at a crosshead speed of 5 mm/min. The filament specimens had a gauge length of 50 mm. At least five tests were performed from which the average and standard deviation of the mechanical properties were evaluated.

3. Results

Melt Shear Viscosity. The capillary rheological data were subjected to Bagley and Weissenberg-Rabinowitsch corrections to determine the true shear rate, shear stress, and shear viscosity [9-11]. Figure 2 shows variation of the shear stress versus shear rate for different temperatures. It can be seen that the shear stress increases with increasing shear rate and decreases with increasing melt temperature.
The variation of the shear stress with the shear rate is usually expressed by the classical power law [10,12]

$$\tau = K\,\dot{\gamma}^{n}, \tag{1}$$

where K is the consistency index, and n is the power low coefficient, which describes the polymer behavior (n<1 indicates shear thinning). The variation of shear stress with shear rate shows a high degree of linearity (in most cases R^2>0.99), indicating non-Newtonian behavior of LDPE and HDPE over the given range of shear rates.
The results in Table 2 indicated that the melt temperature plays an important role in extrusion process.

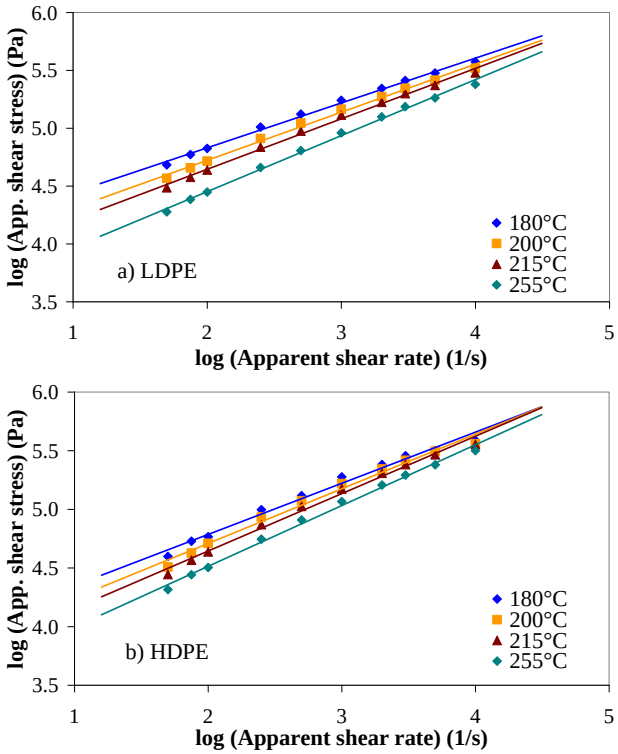

Fig. 2. Melt flow curves at different melt temperatures for a) LDPE and b) HDPE.

Table 2. Power law parameters.

Material	**T (°C)**	**K (Pa s^n)**	**n (-)**	**R^2**
LDPE	180	4.0546	0.3877	0.996
	200	3.8907	0.4158	0.995
	215	3.7729	0.4359	0.996
	255	3.4833	0.4841	0.997
HDPE	180	3.9139	0.436	0.986
	200	3.7768	0.4661	0.987
	215	3.6648	0.4895	0.991
	255	3.4775	0.5182	0.995

Figure 3 illustrates the variation of the shear viscosity with the reciprocal absolute temperature (*1/T*) for different shear rates. In the temperature range of 180 to 255°C, the dependence of shear viscosity on the *1/T* was found to be linear, thus the activation energy for flow, E_a/R, was calculated graphically from the slope of the straight line (see Table 3).

Table 3. Activation energy for flow.

App. shear rate (1/s)	E_a/R (K)	
	LDPE	**HDPE**
100	2397.6	1953.6
500	1950.1	1398.0
1000	1772.5	1227.1
3000	1512.4	614.9

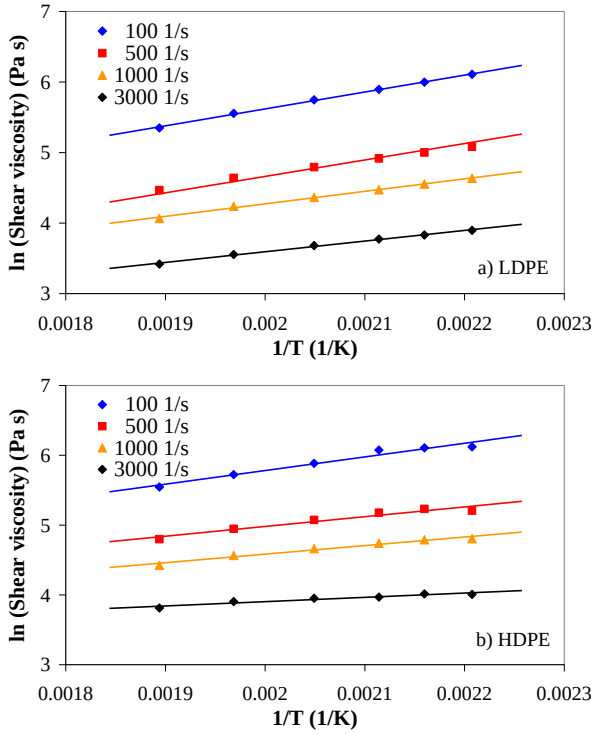

Fig. 3. Effect of melt temperature on the shear viscosity of (a) LDPE and (b) HDPE.

Table 3 clearly shows that the activation energy for flow decreases with increasing shear rate. Although not shown here, the relationship between the activation energy and shear rate is nonlinear. On the other hand, Table 3 indicates that HDPE has lower activation energy when compared with LDPE.

The power law model, in general, is used to describe the flow behavior in the range of medium to high shear rates. However, during the 3D printing, relative low shear rates are expected at the entrance, while the polymer melt reaches high shear rates when passing the printing nozzle [13]. Thus, the Cross and Carreau-Winter viscosity models were used to model the LDPE and HDPE flow behavior [9, 10].

According to the Cross model, the melt shear viscosity at a give shear rate is given by [9, 10].

$$\eta(\dot{\gamma}) = \frac{\eta_0}{1 + \left(\frac{\eta_0 \cdot \dot{\gamma}}{\tau^*}\right)^{1-n}} \tag{2}$$

where η_0 is the zero-shear rate viscosity, τ^* is the critical shear stress at which the onset of shear thinning behavior occurs, and n is the shear-thinning index.
The equation for the Carreau-Winter model is given as follows [9, 10]

$$\eta(\dot{\gamma}) = \frac{\eta_0}{(1 + \lambda\dot{\gamma})^{m_c}}, \tag{3}$$

where λ is the characteristic time, i.e. the inverse of the shear rate at which the shear-thinning behavior begins, m_c is the increase of the viscosity function, $m_c \approx n\text{-}1$. This model is appropriate in the low to medium shear rate ranges, as in the case for filament extrusion.

The predicted values for the melt shear viscosity of LDPE and HDPE using the Cross model are shown in figure 4, while figure 5 shows the predicted values for the melt shear viscosity using the Carreau-Winter model. As expected, the melt shear viscosity decreases with increasing both shear rate and melt temperature. Moreover, both polymers display shear thinning behavior at high shear rates.

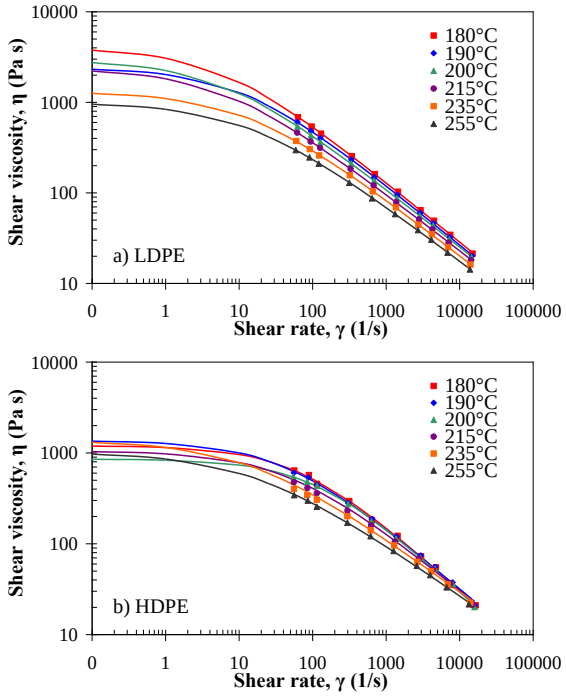

Fig. 4. Melt shear flow curves for (a) LDPE and (b) HDPE. Solid line indicates the Cross model.

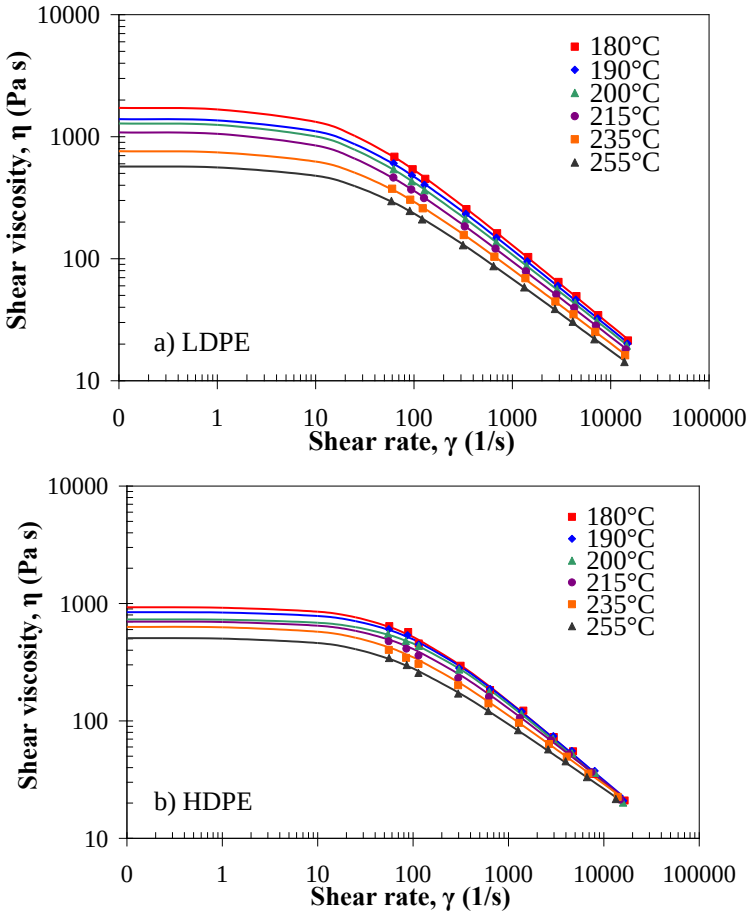

Fig. 5. Melt shear flow curves for (a) LDPE and (b) HDPE.
Solid line indicates the Carreau-Winter model.

Figure 6 compares the flow curves predicted by Cross (solid line) and Carreau-Winter (the dotted line) models at 215°C. As can be seen in figure 6, in the domain of high shear rates, both models predict very well the experimental data, while in the low shear rate region the Carreau-Winter model predicts lower values for the η_0. However, it is important to note that, at shear rates lower than 100 s^{-1}, the viscosity predictions must be treated with great caution because no experimental data were available.

For each polymer, a master curve was generated using the Time-Temperature-Superposition (*TTS*) principle [10]. The parameters for the Cross and Carreau-Winter models obtained using the master curve are listed in Table 4. The master curves will allow determination of the melt shear viscosity over a wide range of shear rates for a particular temperature.

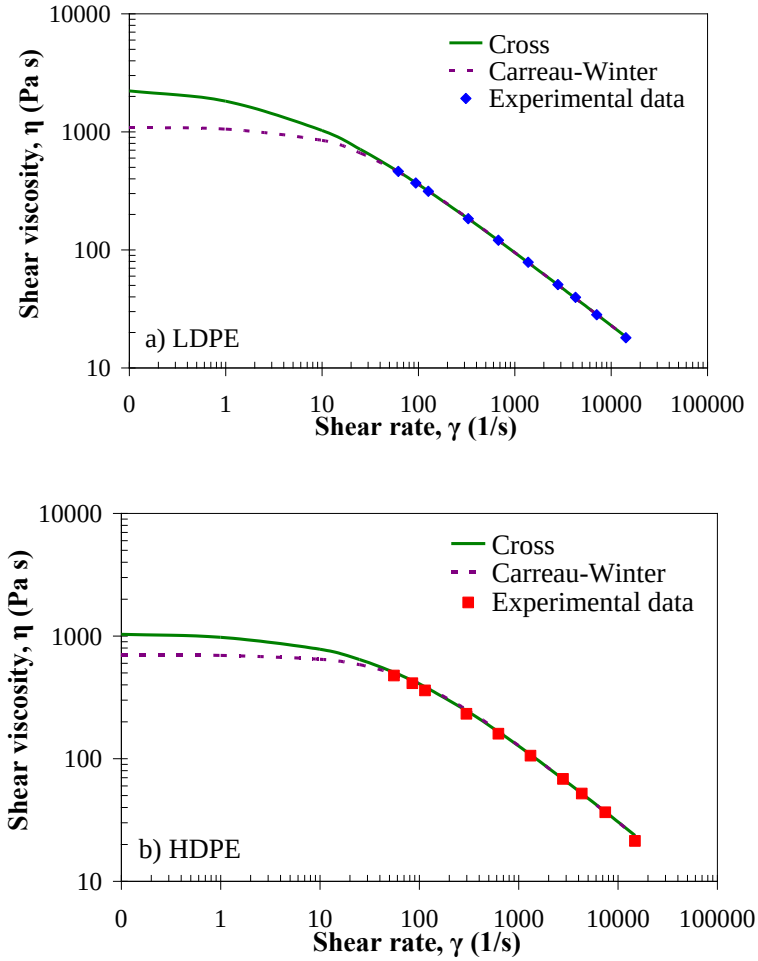

Fig. 6. Comparison between Cross and Carreau-Winter viscosity at 215°C.

Table 4. Cross and Carreau-Winter parameters at a reference temperature of 200°C

Model	Parameter	LDPE	HDPE
Cross	η_0 (Pa·s)	2066.664	1170.074
	τ^* (Pa)	25332.168	55232.418
	n	0.343	0.328
	R^2	0.999	0.998
Carreau-Winter	η_0 (Pa·s)	1286.808	780.283
	λ (s)	0.048	0.013
	m_c	0.638	0.661
	R^2	0.999	0.997

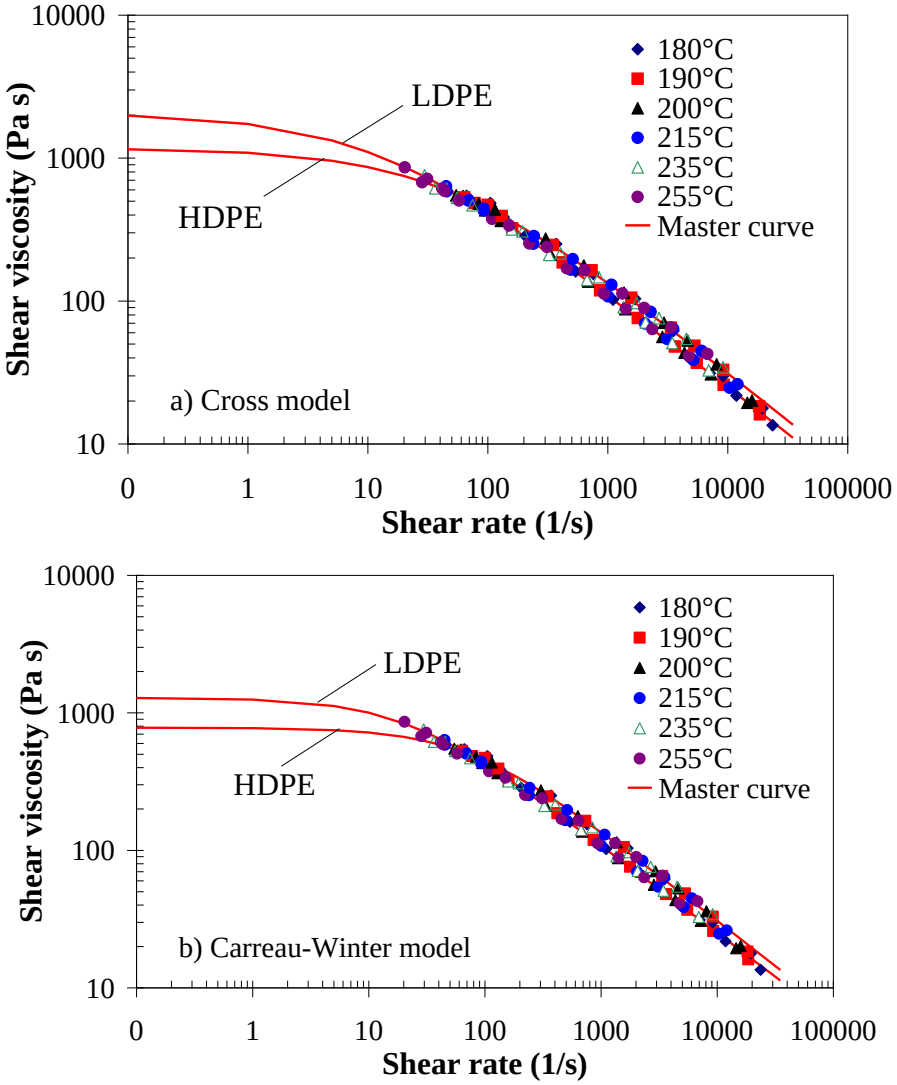

Fig. 7. Master curve of LDPE and HDPE at a reference temperature of 200°C: (a) Cross and (b) Carreau-Winter models.

Filament extrusion. Figure 8 shows the variation of the filament diameter over time for different extrusion conditions. These measurements were automatically recorded by the optical sensor of the extruder. The solid lines indicate the acceptable diameter tolerance for the 3D printing filament, i.e. ±0.05 mm.

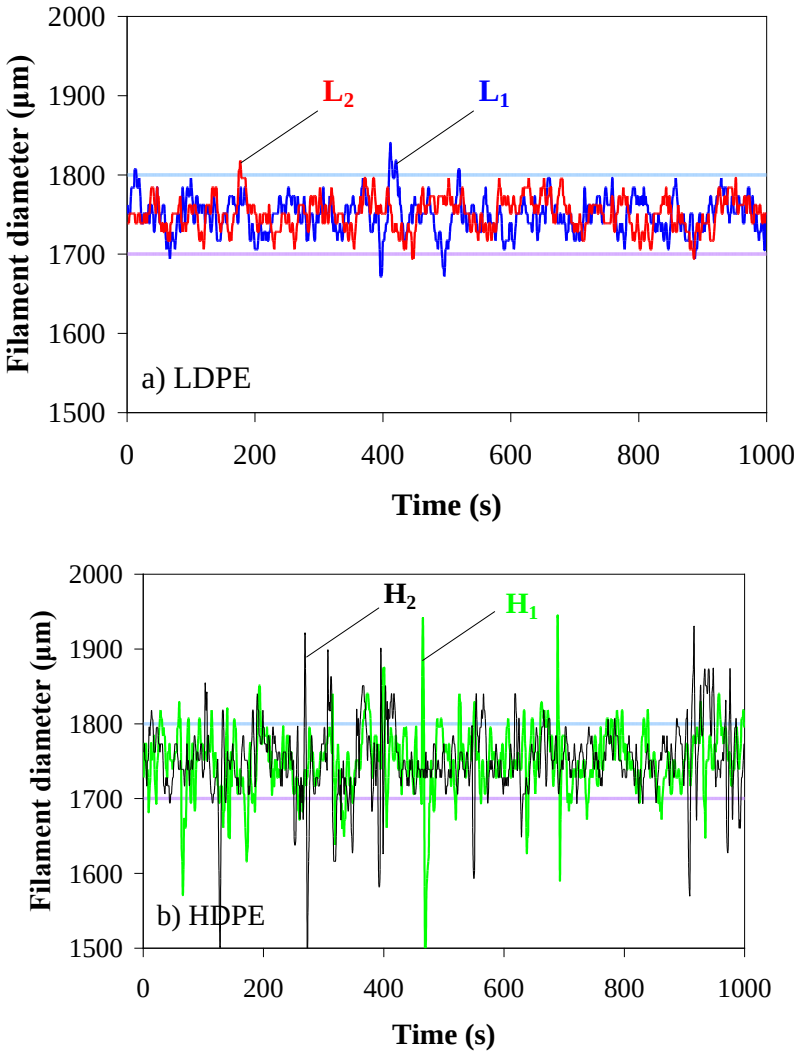

Fig. 8. Filament diameter vs. time for LDPE and HDPE.

It can be seen that the filament diameter varies during the extrusion process. However, the largest variations were observed for the HDPE, particularly for L_2 filament which exceeds the acceptable tolerance. Moreover, for L_2 and H_2 processing conditions the filament does not have a constant circular shape across the filament length. The variation of filament diameter can be caused by different factors, such as the shape of the pellets, viscosity, temperature, speed, etc. [14].

Figure 9 shows the variation of the extrusion speed versus extrusion time. It can be seen that the speed used for HDPE varies less than that for LDPE.

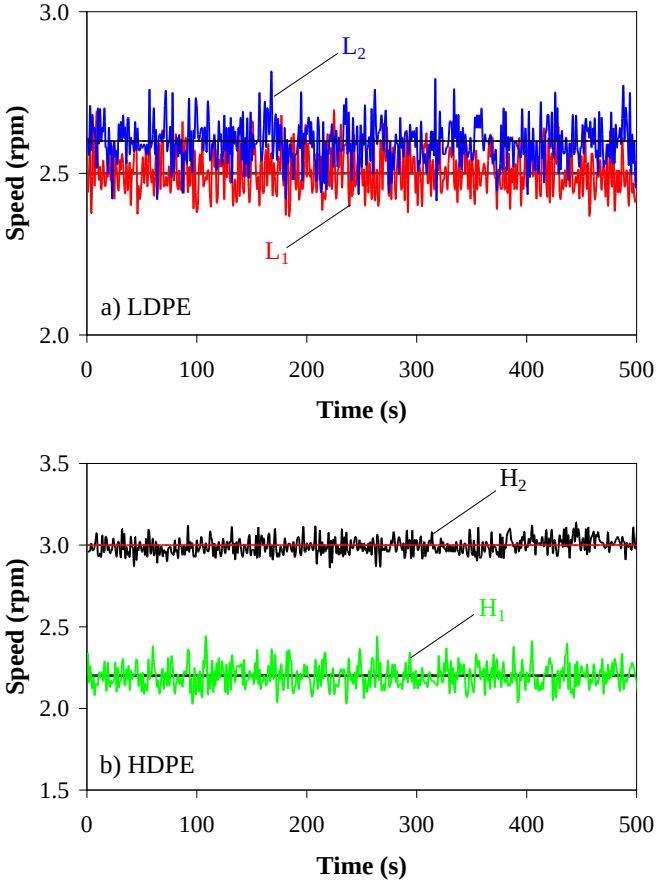

Fig. 9. Speed vs time during extrusion of the LDPE and HDPE.

Images of the LDPE and HDPE filaments are presented in figures 10 and 11, respectively. For LDPE, as shown in fig. 10b, the L_1 filament with the average diameter of 1.748±0.02 mm displays smooth surface with very fine indentations along the filament length, but the outcome was satisfactory in term of diameter tolerance and filament roundness (less then ±0.05 mm). On the other hand, the indentations became less visible with increasing T_1 and T_2 temperatures and speed (see L_2 conditions in Table 1), however, the filament cross-section changed from circular to oval, as shown in fig. 10a.

For HDPE, as shown in figure 11, the filaments display bumps. However the size of the bumps depends on the extrusion conditions. It is important to note that the bumps are detected by the optical sensor of the extruder and interpreted as a variation in diameter. For H_1 conditions, the HDPE filament is round shaped and uniform with an average diameter of 1.75 ±0.044 mm.

However, with increasing the speed and T_1 and T_2 temperatures of the extruder results in a filament with flatted oval cross-section.

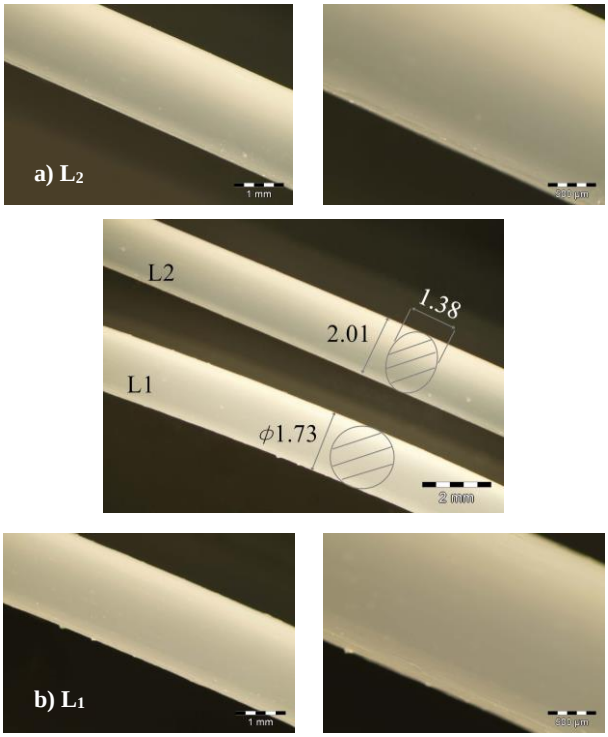

Fig. 10. Images of the LDPE filaments.

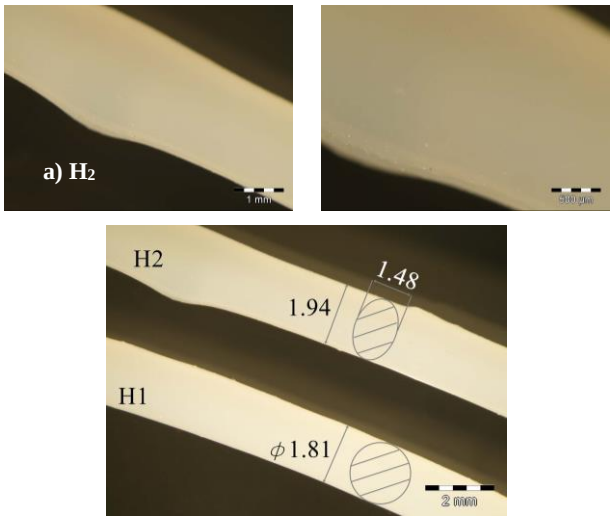

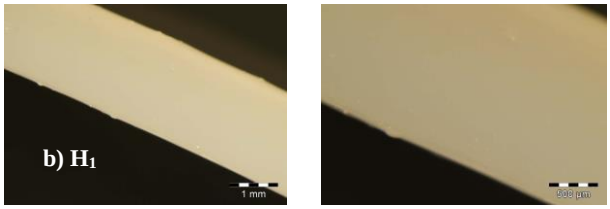

Fig. 11. Images of HDPE filaments.

Based on the experimental results, it was concluded that the optimum extrusion parameters are L_1 and H_1. For these parameters, the filaments are satisfactory in terms of diameter tolerance, filament roundness and surface quality.

Mechanical properties. Figure 12 shows the representative stress-strain curves for LDPE and HDPE filaments corresponding to L_1 and H_1 extrusion conditions. The elastic moduli, stress at yield and stress at break are given in Table 5. It can be seen that the HDPE exhibits a typical elasto-plastic behavior with yielding, softening and hardening. On the other hand, the LDPE filament exhibits a different behavior without softening upon reaching the yielding point.

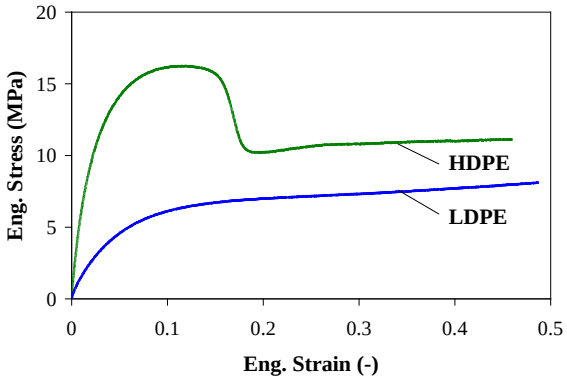

Fig. 12. Stress-strain curve for LDPE and HDPE filament.

Table 5. Mechanical properties of the filaments

Material	E (MPa)	Stress @ yield (MPa)	Stress @ Break (MPa)
LDPE	165.53±20.81	5.76±0.23	7.43±0.64
HDPE	730.57±43.85	16.24±0.72	10.61±0.45

Figure 12 and Table 5 indicate that HDPE filaments exhibit higher mechanical properties than LDPE filaments due to higher crystallinity [8].

Based on the experimental data it can be concluded that HDPE filaments can be used for 3D printing of parts that require higher mechanical properties, while LDPE filaments for 3D printing of parts that require flexibility.

4. Conclusions

In this paper, the feasibility of using low and high density polyethylenes as a printable 3D filament was investigated. LDPE and HDPE were extruded under different processing conditions to form standard 1.75 mm diameter filaments. The effect of extrusion parameters on the filament surface and diameter was investigated by optical microscopy. In addition, the melt properties were determined by capillary rheology.

Based on the experimental results the following conclusions are drawn:

(i) Round and smooth HDPE and LDPE filaments with diameter of 1.75 ±0.044 mm and 1.748±0.02 mm, respectively, were produced;

(ii) The LDPE filaments have shown major differences compared to HDPE filaments in terms of mechanical properties.

Experimental results showed that the LDPE and HDPE are suitable for manufacturing 3D printing filaments if the extrusion parameters are adequately selected. However, further research on filament extrusion process and 3D printing properties is needed.

References

[1] Stansbury J.W., Idacavagec M.J., *3D printing with polymers: Challenges among expanding options and opportunities*, Dental Materials, **32**, 2016, p. 54-64.

[2] Wang X., Jiang M., Zhou Z., Gou J., Hui D., *3D printing of polymer matrix composites: A review and prospective*, Composites Part B Engineering, **110**, 2017, p. 442-458.

[3] Parandoush P., Lin D., *A review on additive manufacturing of polymer-fiber composites*, Composite Structures, **182**, 2017, p. 36-53.

[4] Dizon J.R.C., Espera Jr. A.H., Chen Q., Advincula R.C., *Mechanical characterization of 3D-printed polymers*, Additive Manufacturing, **20**, 2018, p. 44-67.

[5] Ngo T. D., Kashani A., Imbalzanoa G., Nguyena K. T.Q., Hui D., *Additive manufacturing (3D printing): A review of materials, methods, applications and challenges*, Composites Part B, **143**, 2018, p. 172 - 196.

[6] https://en.reset.org/knowledge/3d-printing-adding-sustainable-dimension-modern-life-02262018

[7] Statistical data from https://www.statista.com

[8] Sandu I.L., *Contributions to thin - walled injection molding polymer parts*, PhD thesis, 2014.

[9] Lima P., Magalhaes da Silva S.P., Oliveira J., Costa V., *Rheological properties of ground tyre rubber based thermoplastic elastomeric blends* – Polymer Testing, **45**, 2015, p. 58-67.

[10] Morrison F.A., *Understanding rheology* – Oxford University Press, 2001.

[11] Mitsoulis E., Hatzikiriakos S.G., Christodoulou K., Vlassopoulos D., *Sensitivity analysis of the Bagley correction to shear and extesnional rheology*, Rheologica Acta, **37**, 1998, p. 438-448.

[12] Liang J.Z., Chen C.Y., Zou S.Y., Tsui C.P., Tang Y., Zhang S.D., *Melt flow behavior of polypropylene composites filled with multi-walled carbon nanotubes during extrusion*, Polymer Testing, **45**, 2015, p. 41-46.

[13] Turner N. Brian, Strong Robert and Gold A. Scott, *A review of melt extrusion additive manufacturing processes: I. Process design and modeling*, Rapid Prototyping Journal, **20**/3, 2014, p. 192–204.

[14] Filament extrusion support and tips from https://www.support.3devo.com/